JOURNAL OF NEUROTRAUMA 35:1737–1744 (August 1, 2018)
© Mary Ann Liebert, Inc.
DOI: 10.1089/neu.2017.5444

Differential Adaptations of the Musculoskeletal System after Spinal Cord Contusion and Transection in Rats

Ching-Yi Lin,[1] Charlie Androjna,[2] Richard Rozic,[2] Bichtram Nguyen,[1] Brett Parsons,[1] Ronald J. Midura,[2] and Yu-Shang Lee[1]

Abstract

Spinal cord injury (SCI) causes impaired neuronal function with associated deficits in the musculoskeletal system, which can lead to permanent disability. Here, the impact of SCI on *in vivo* musculoskeletal adaptation was determined by studying deficits in locomotor function and analyzing changes that occur in the muscle and bone compartments within the rat hindlimb after contusion or transection SCI. Analyses of locomotor patterns, as assessed via the Basso, Beattie, and Bresnahan (BBB) rating scale, revealed that transection animals showed significant deficits, while the contusion group had moderate deficits, compared with naïve groups. Muscle myofiber cross-sectional areas (CSA) of both the soleus and tibialis anterior muscles were significantly decreased three months after contusion SCI. Such decreases in CSA were even more dramatic in the transection SCI group, suggesting a dependence on muscle activity, which is further validated by the correlation analyses between BBB score and myofiber CSA. Bone compartment analyses, however, revealed that transection animals showed the most significant deficits, while contusion animals showed no significant differences in the trabecular bone content within the proximal tibia compartment. In general, values of bone volume per total bone volume (BV/TV) were similar across the SCI groups. Significant decreases were observed, however, in the transection animals for bone mineral content, bone mineral density, and three-dimensional trabecular structure parameters (trabecular number, thickness, and spacing) compared with the naïve and contusion groups. Together, these findings suggest an altered musculoskeletal system can be correlated directly to motor dysfunctions seen after SCI.

Keywords: contusion; musculoskeletal adaptation; spinal cord injury; transection

Introduction

Spinal cord injury (SCI) results in the progressive loss of skeletal muscle (sarcopenia) and bone (osteopenia), leading to functional deficits and profound consequences for quality of life.[1,2] Over the last decade, there has been increasing awareness that skeletal muscle and bone tissues interact locally via direct mechanical interactions and reciprocal biochemical cross-talk mechanisms.[3] While muscle loss typically precedes bone loss in disuse situations because of the difference in remodeling rates for these two tissue types, it is not entirely clear whether the earlier presence of sarcopenia only influences osteopenia as a result of a decline in mechanical loading on the bone because of decreased muscle contraction forces, or if there are other reciprocal signaling mechanisms between these two tissues that are in close proximity to each other. Recent evidence suggests that the earlier loss of muscle tissue may exert other influences that contribute to bone loss.[3,4] One area of study needing further investigation is assessing the relationship between sarcopenia and osteopenia after SCI.

SCI in humans is more prevalent in adults than in children,[5] and pediatric patients incurring SCI typically have better neurological recovery than adults.[6] In adults, SCI leads to progressive and profound loss of skeletal muscle and bone tissues in the lower extremities.[7,8] Moreover, it has been reported that the rates of bone and muscle loss sublesional to the SCI site are typically greater than those for bone and muscle sites that are supralesional.[7,8] It has been suggested that bone loss in adult humans after SCI is thought to be an effect of enhanced resorption activities, with little to no changes in bone formation activities.[9–11]

A rodent pre-clinical model of SCI reporting locomotion levels assessed by the Basso, Beattie, and Bresnahan (BBB) scale demonstrated a threshold of footfall stepping activities that distinguished those rats manifesting a loss of bone mass over an eight-week testing period versus those rats that did not exhibit major loss of bone mass.[11] Nevertheless, this study used young growing rats, and it is not clear whether this footfall stepping threshold would extend to skeletally mature rats. Thus, the hypothesis that mechanical loading of the lower extremities early after SCI can mitigate the subsequent

Departments of [1]Neurosciences and [2]Biomedical Engineering, Lerner Research Institute, Cleveland Clinic, Cleveland, Ohio.

rate of bone loss has merit, but it requires further investigation using skeletally mature animals.

Most pre-clinical studies published to date have not tested this hypothesis rigorously and are also limited by using young, growing rats and not skeletally mature rodents to assess loss of bone mass. Young growing rodents experience a rapid cessation of bone growth within the first few weeks after SCI, followed by a more gradual loss of existing bone tissue (or resorption of existing bone) over several months thereafter.[12] Also, unilateral sciatic neurectomy in growing rats was reported to inhibit bone growth and to reduce trabecular bone mass mainly within the first four weeks after neurectomy.[13] Thus, a study design using young, growing rodents could not distinguish the negative impacts of SCI slowing or stopping bone growth from that of enhancing resorption of pre-existing bone tissue.

Skeletal maturity in the rat begins at about six to seven months of age, and roughly 80–85% of long bone growth is complete by three to four months of age.[14–16] One published study demonstrated that four-month–old male Fischer rats exhibited loss of femur bone mass after a 25 g-cm impact-force contusion SCI over a 16-week test period.[17] This particular study did not assess BBB locomotion scores and did not assess changes in skeletal muscle mass during this testing period. As a result, cross-correlation between the extent of skeletal muscle loss and that of bone loss in the lower extremity could not be assessed. Moreover, that study focused on a single SCI approach and could not assess whether a threshold level of footfall stepping would be apparent in skeletally mature rats.

The current study hypothesized that the presence of footfall stepping early after SCI would slow the subsequent rates of muscle and bone loss in the hindlimbs of rats nearing skeletal maturity. We tested this hypothesis in skeletally mature rats using two different SCI models and assessed BBB locomotion scores, skeletal muscle loss using histology, and bone loss using micro-computed tomography (micro-CT) three months after SCI.

Methods

Animal groups and experimental design

Twenty-five female Sprague-Dawley (SD) rats at three months of age (225–250 g; Harlan, San Diego, CA) were divided randomly into three groups: (1) age-matched control group (naïve; $n=4$), (2) spinal cord contusion (contusion; $n=10$), (3) spinal cord transection (transection; $n=11$). All rats were purchased nulliparous at $\sim$three months of age at the beginning of the study and were tested over three months (animals were six months old at the study end-point). The importance of using nulliparous female rats to study cancellous bone assessments has been established previously by reports showing that repeated cycles of pregnancy and lactation in proven breeder female rats alters their bone structure and material properties, making them inappropriate for use as age-matched controls in the current study design.[18]

All procedures involving animals followed National Institutes of Health guidelines and were approved by the Institutional Animal Care and Use Committee of the Cleveland Clinic. Animals were housed in ventilated humidity- and temperature-controlled (23–25°C) rooms with a 12:12-h light-dark cycle and standard rodent chow and water available *ad libitum*.

Contusion SCI

Rats were acclimated to the animal resource center, behavior assessments, and experimental handlers before starting the study. Rats were anesthetized under 2% isoflurane mixed with oxygen. The musculature was cut from T7–T9, and the dorsal surface of T8 was exposed by laminectomy. The vertebral column was stabilized by clamping the T7 and T9 vertebral bodies with forceps fixed to the base of the Infinite Horizon Impact (IH impactor, Precision Systems and Instrumentation, LLC). The animals were situated on the platform, and the 2.5-mm stainless steel impactor tip was positioned over the midpoint of T8 and impacted with a 250 kDyne force. Monofilament sutures (4-0) were used to close the skin and musculature. A force/displacement graph was used to monitor impact consistency, and any animal that exhibited an abnormal impact graph or greater than 10% deviation from 250 kDyne was excluded immediately from the study. Manual bladder expression was performed twice daily throughout the three-month experimental period.

Transection SCI

Before the surgical procedure, rats were anesthetized using 2% isoflurane mixed with oxygen. Animals were maintained on a heating pad, and rectal temperature was monitored and maintained during the procedure. Bipolar electrocauterization was used to minimize bleeding in some animals. A laminectomy was performed as described above for contusion SCI, followed by complete transverse cuts of the spinal cord at the T8 level. A surgical microscope was used to ensure the complete removal of neural tissue, including fiber bundles. The muscle and skin layers were closed with 4-0 sutures. Bladders were expressed manually twice per day throughout the three-month experimental period.

Open-field locomotion assessments

Locomotor function was evaluated using the BBB rating scale[19] ranging from 0 to 21. Assessments were performed before SCI and weekly thereafter throughout the entire experimental period as described previously. Scoring was undertaken by two independent examiners who were trained initially on the BBB scoring system and were blinded regarding animal groups.

Myofiber cross-sectional area (CSA)

At the experimental end-point, each rat was euthanized and perfused (intracardiac) with a 4% paraformaldehyde solution. Both the soleus muscle and the tibialis anterior muscle were harvested. Samples of the muscle blocks were sectioned in a cryostat into 8-μm thick cross-sectional pieces and mounted directly onto gelatin-coated slides. Hematoxylin and eosin (H&E) staining was used to visualize the myofibers of the muscle. Images of the sections were taken using a Leica DM6000 (DM6000; Leica Microsystems, Buffalo Grove, IL). The CSA of approximately 200 randomly selected myofibers from each muscle per animal were measured using MATLAB R2016a (The MathWorks, Inc., Natick, MA).

Bone structural assessments

Bone structure and mineral density metrics were evaluated using micro-CT. Micro-CT data were acquired post-mortem on a region of interest (ROI) from midfemur to the tibia-fibula synostosis in isolated hind-limbs at 20 μm isotropic voxel resolution (GE Locus, Trifoil, Inc.). Post-acquisition reconstruction (GE Reconstruction Utility software), micro-CT data volumes were calibrated/normalized further using solid water phantoms that were scanned in conjunction with the *ex vivo* specimens. The phantoms are representative of spongy, trabecular (800 mg/cm^3 hydroxyapatite), and cortical (1250 mg/cm^3 hydroxyapaptite) bone mineral content and density. The micro-CT volume grayscale values (correlated to Hounsfield units) were normalized to these standard phantoms so that a standard grayscale threshold level could be applied to all volumes for trabecular bone metrics (HUCalibrate_v1.1 software, Image-IQ Inc., Cleveland OH; http://image-iq.com/).

Trabecular bone structural and material metrics were determined from a 3.0-mm ROI in the proximal tibia starting approximately 1.8-mm below the growth plate (Fig. 1). All volumes were registered into the same orientation and three-dimensional (3D) space, allowing for the same ROI to be cropped from the full tibia bone between animals. Subsequently, all volumes were cropped to a 3-mm segment and the cortical volume masked along the cropped length as represented in the figure. Outcome values were determined from the 16-bit 3D volumes, specifically within the trabecular compartment, thresholded at a uniform grayscale value of 1800, and post-processed using BoneAnalysis_v5.1 software (Image-IQ Inc., Cleveland OH) for structural and mineral density outcome metrics.

Statistical analysis

All BBB scores, CSA values of muscles, and bone structure and mineral density metric values were reported as mean ± standard error of the mean (SEM) for each group. Statistical significance was set at $p < 0.05$ and assessed by analysis of variance (one-way ANOVA), followed by Tukey *post hoc* tests between groups using the statistical analysis software GraphPad Prism 5.0 (GraphPad, La Jolla, CA).

Pearson correlation analyses were also performed to determine the relationship between locomotor function (BBB scores) and CSA values of muscle, as well as between BBB scores and mineral density metric values of bone. All analyses were performed using the statistical analysis software GraphPad Prism 5.0 (GraphPad).

Results

Comparison of contusion SCI impactor devices

Figure 2 shows a comparison of impact force between the IH impactor used in this study and that of the New York University (NYU) impactor used in several previous reports. The impact force produced by the IH impactor at 250 kDyne roughly equates to somewhere between 6.25 to 12.5 g-cm when using the NYU impactor. These data allow for a direct comparison between these two devices at various impact settings and confirm that the IH impactor used in this study is generating a lower impact force than what has been reported in several previous rat SCI studies (typically 25 g-cm or higher).

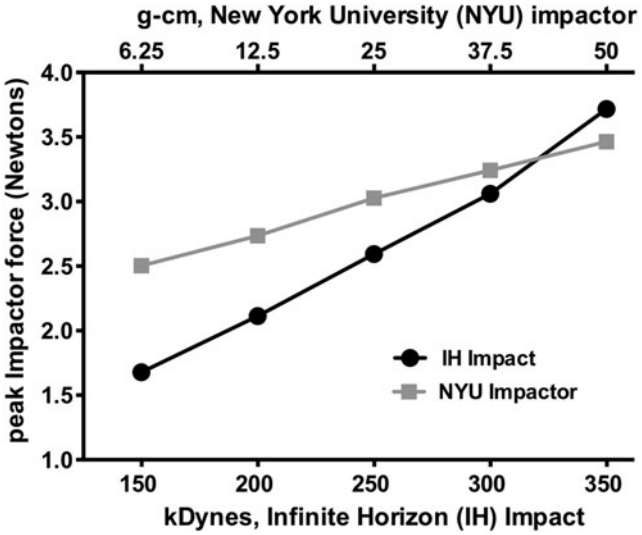

FIG. 2. Force comparison between the Infinite Horizon (IH) and New York University (NYU) impactors. We recorded force data using custom software built on simVITRO® LabVIEW packages (Cleveland Clinic, Cleveland, OH). The impactor struck a tissue surrogate laid on top of a nano17 force/torque sensor (ATI, Apex, NC). The forces were recorded at 20,000 Hz. The peak force was recorded and compared with each programmed impactor force. Data are presented as mean ± standard error of the mean (five trials run per impactor force). Top and bottom X-axes represent the impactor force programmed by NYU (g-cm) and IH (kDynes) impactors, respectively. Plotted on the Y-axis is the average peak impactor force achieved for each programmed impactor force.

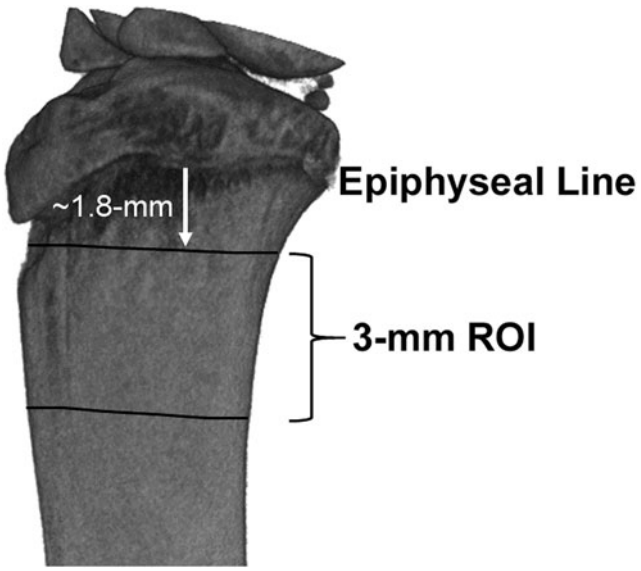

FIG. 1. Representative micro-computed tomography volume of the proximal tibia that depicts the region-of-interest (ROI) over which bone structural and mineral density metrics were determined. The ROI was 3 mm in length, beginning approximately 1.8 mm below the epiphyseal line of the tibia.

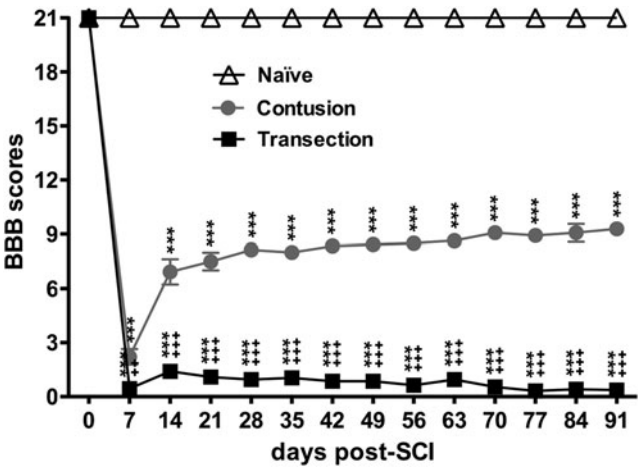

FIG. 3. Locomotor assessments after spinal cord injury (SCI) using the Basso, Beattie, and Bresnahan (BBB) scale. BBB scores of the contusion animals were significantly greater than those of the transection animals, but significantly smaller than those of the naïve animals. Graph shows quantification of mean ± standard error of the mean values. Two-way repeated measures analysis of variance with Bonferroni *post-hoc* for multiple comparisons. *** $p < 0.005$ vs. naïve group; $^{++}$ $p < 0.01$, $^{+++}$ $p < 0.005$ vs. contusion group.

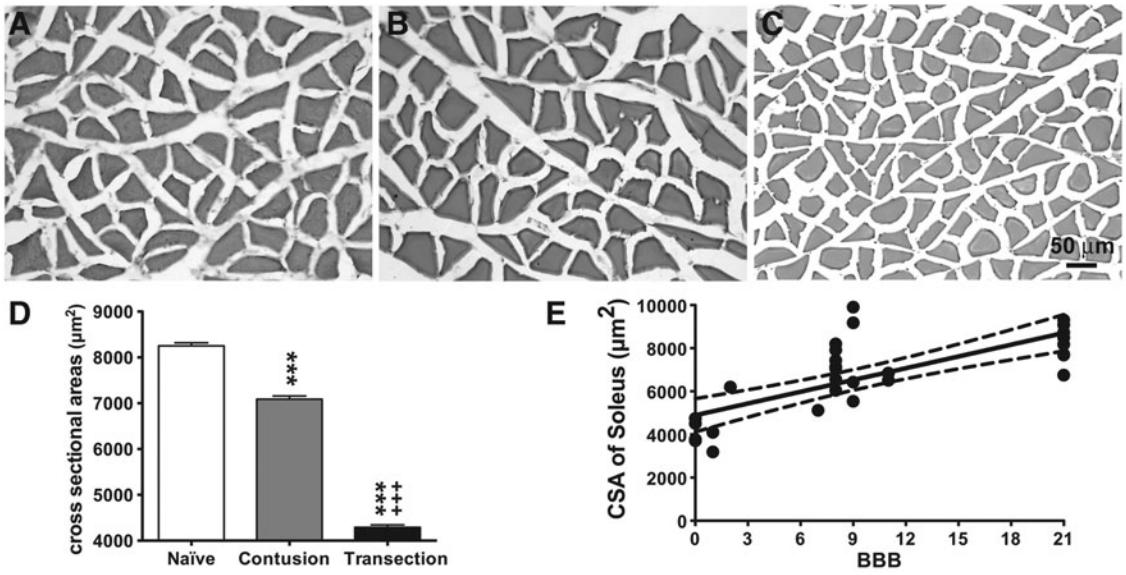

FIG. 4. Cross-sectional area (CSA) of soleus myofibers after SCI. Representative sections stained with hematoxylin and eosin from the naïve group (**A**), spinal cord contusion group (**B**), and spinal cord transection group (**C**) are depicted. Scale bar, 50 μm. (**D**) Bar graph showing mean ± standard error of the mean values of CSA in each group. The mean myofiber CSA of the contusion group was significantly smaller than that of the naïve animals, but was significantly greater than that of the transection animals. *** $p < 0.005$ vs. naïve group; $^{+++}$ $p < 0.005$ vs. contusion group; two-way analysis of variance with Bonferroni *post-hoc* for multiple comparisons. (**E**) Correlation analyses between the Basso, Beattie, and Bresnahan (BBB) and average myofiber CSA in the naïve and SCI (contusion and transection) groups. Data are presented as X-Y paired, with linear regression (solid line) and 95% confidence limits (dashed lines) of the fit.

Locomotion is impaired after SCI

At seven days after SCI, mean BBB scores in the transection and contusion groups were decreased significantly to 0.25 and 2.93, respectively, indicating significant differences between groups in terms of injury severity (transection vs. contusion) (Fig. 3). A significant improvement was found beginning from seven to 14 days, while a trend (but no statistically significant difference over time) toward better recovery from 14 to 91 days was seen in rats with contusion SCI with scores ranging from 6.93 to 9.23,

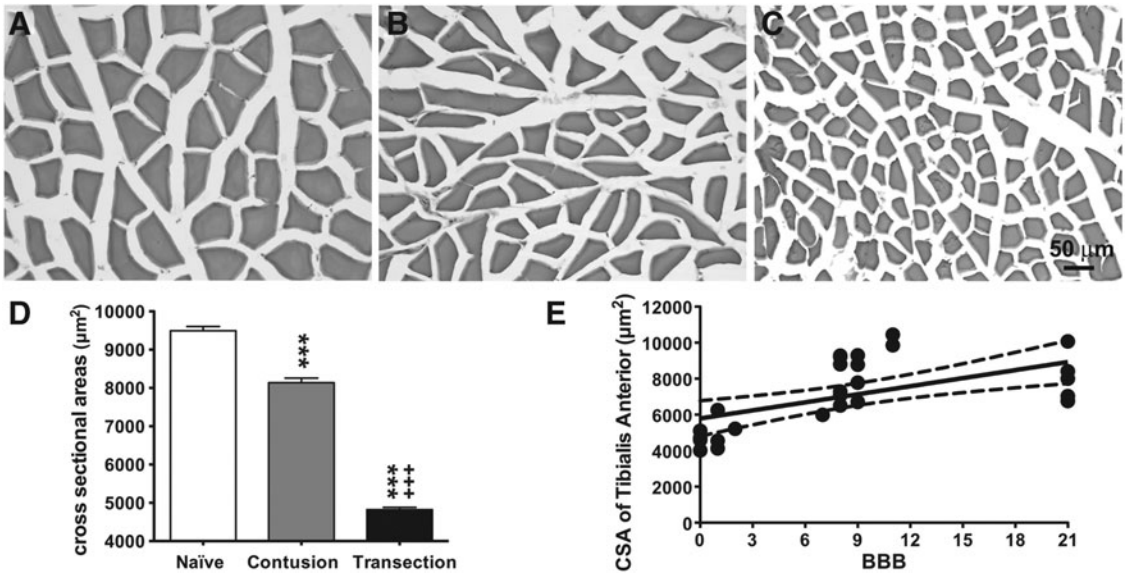

FIG. 5. Cross-sectional area (CSA) of tibialis anterior myofibers after spinal cord injury (SC)I. Representative sections stained with hematoxylin and eosin from the naïve group (**A**), spinal cord contusion group (**B**), and spinal cord transection group (**C**) are depicted. Scale bar, 50 μm. (**D**) Bar graph showing the effects (mean ± standard error of the mean values) of SCI on the CSA of the tibialis anterior myofibers. CSA was significantly decreased by contusion injury compared with the naïve group. Spinal cord transection resulted in a significantly lower CSA when compared with the contusion group. *** $p < 0.005$ vs. naïve group; $^{+++}$ $p < 0.005$ vs. contusion group; two-way analysis of variance with Bonferroni *post-hoc* for multiple comparisons. (**E**) Correlation analyses between the Basso, Beattie, and Bresnahan (BBB) and average myofiber CSA in the naïve and SCI (contusion and transection) groups. Data are presented as X-Y paired, with linear regression (solid line) and 95% confidence limits (dashed lines) of the fit.

indicating that the animals could either extensively move all three joints of a hindlimb (BBB 6.93) or stepping with limited weight support (BBB 9.23) (Fig. 3). In contrast, at seven to 91 days after transection SCI, mean BBB scores were similar (ranging from 0.45 to 0.36) over time, indicating permanent hindlimb paralysis with only minimal activity (Fig. 3).

Adaptation of soleus and tibialis anterior muscles

Next, we examined the changes in muscles of hindlimbs after SCI. After staining every tenth section with H&E (at least 10 sections per animal), we determined the CSA of the randomly selected myofibers from muscles including the soleus (the flexor muscle of the ankle) and the tibialis anterior (the extensor muscle at the hindlimb).

As shown in Figure 4, spinal cord transection produced a significant loss in soleus myofiber CSA (Fig. 4C, D). The mean CSA of the soleus myofibers was $4292 \pm 53.5\,mm^2$ in the transected animals, which was significantly less than that of the naïve group ($8251 \pm 66.7\,mm^2$), representing a loss of $\sim$48% of myofiber CSA. In contrast, contusion caused a relatively moderate decrease ($\sim$14% loss) in the mean CSA of soleus myofibers ($7088 \pm 68.8\,mm^2$) compared with the naïve group (Fig. 4B, D), which was $\sim$65% greater than that of the transection group ($p < 0.005$).

A similar adaptation trend was seen in tibialis anterior myofibers (Fig. 5). Contusion SCI ($8138 \pm 117.7\,mm^2$) caused significant loss (17%) in CSA of tibialis anterior myofibers compared with the naïve group ($9494 \pm 112.7\,mm^2$) (Fig. 5B, D). Such loss was even more significant in the transection group ($4821 \pm 61.47\,mm^2$), which was a $\sim$49% loss when compared with the naïve group (Fig. 5C, D).

Importantly, correlation plots of BBB scores with myofiber CSA values demonstrate a linear relationship (Fig. 4E, 5E), indicating that transection SCI animals with less hindlimb mobility (Fig. 3) showed greater losses in myofiber CSA than contusion SCI animals (Fig. 4E vs. 5E) with more hindlimb mobility (Fig. 3). These results are consistent with the observation that individual muscle bundle

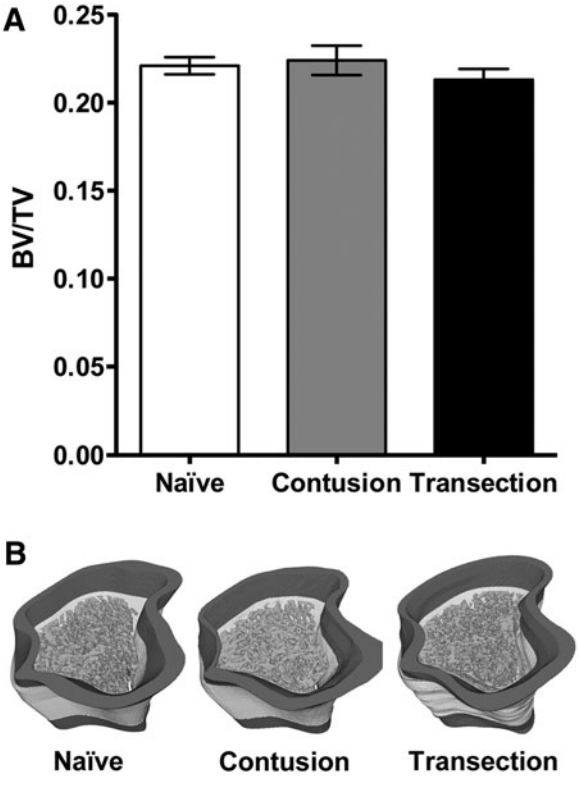

FIG. 6. Micro-computed tomography image analysis of the rat proximal tibia. (**A**) The bone volume fraction (BV/TV) determined within the trabecular bone compartment of the proximal tibia for the naïve, contusion, and transection groups (mean ± standard error of the mean). Statistical analyses (one-way analysis of variance, *post-hoc* Tukey) determined no statistically significant differences between any of the groups. (**B**) Representative three-dimensional (3D), computer-generated 16-bit volumes depicting BV/TV region of interest (ROI) evaluated for the naïve, contusion, and transection groups; the dark gray mask represents the original cropped volume ($\sim$1.8-mm below the epiphyseal line), the white mask represents the 3-mm high ROI evaluated, and the gray mask inside the cortical boundary represents the generated 3D trabecular structure.

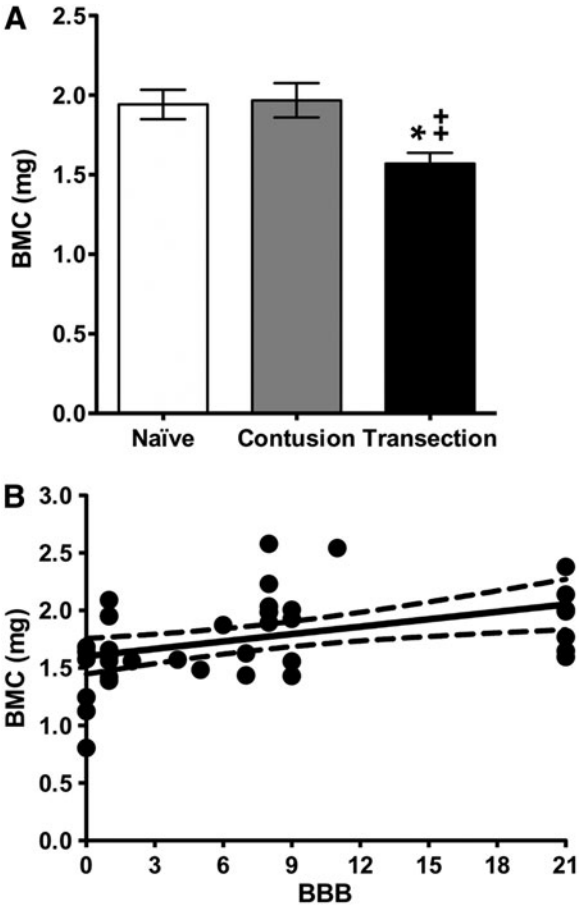

FIG. 7. (**A**) Bone mineral content (BMC, mg calcium) determined within the trabecular bone compartment of the proximal Tibia for the naïve, contusion, and transection groups (mean ± standard error of the mean). Statistical analyses (one-way analysis of variance, *post-hoc* Tukey) indicated a significant difference (* $p < 0.05$) between the transection and naïve groups as well as a significant difference ($^{++}$ $p < 0.01$) between the transection and contusion groups. (**B**) Correlation analyses between the Basso, Beattie, and Bresnahan (BBB) and BMC in the naïve and SCI (contusion and transection) groups. Data are presented as X-Y paired, with linear regression (solid line) and 95% confidence limits (dashed lines) of the fit.

contractile areas were smaller in the transection versus contusion model (Fig. 4B vs. 4C and 5B vs. 5C). Therefore, while SCI induced sarcopenia in both muscle types, the type of SCI model (contusion vs. transection) resulted in different extents of muscle atrophy.

Bone structural assessments

Trabecular bone volume fraction data (bone volume per total bone volume or BV/TV) (Fig. 6A) from standardized ROIs (Fig. 1) were: naïve (22% ± 0.4%), contusion (22% ± 0.8%), and transection (21% ± 0.6%). Statistical analyses indicated no significant differences in BV/TV when contusion or transection groups were compared with the naïve group, and, similarly, no significant differences were found between the contusion and transection groups. Further, qualitative review of the 3D segmented trabecular masks overlaid onto the bone micro-CT image volumes further established that there were no observable volumetric differences between the naïve and SCI groups (Fig. 6B).

Bone mineral content (BMC, mg calcium) data are depicted in Figure 7A for the naïve (1.9 ± 0.09), contusion (2.0 ± 0.11), and transection groups (1.6 ± 0.07). Statistical analyses indicated that the transection group exhibited significantly reduced BMC values (~20–25%) when compared with that of either the naïve or contusion groups. Correlation analyses between the BBB scores and BMC values are depicted in Figure 7B. These analyses show that the strength of association between BBB scores and BMC is moderate (r = 0.446) and that the correlation coefficient is significantly different from zero ($p < 0.002$). We can only say, however, that 20% (0.446^2) of the variation in BMC values can be explained by mechanical unloading, as represented by the decreasing locomotion function because of severity of the injury.

Bone mineral density (BMD, mg calcium/cm^3) data are depicted in Figure 8A for the naïve (530 ± 18), contusion (513 ± 12), and transection groups (368 ± 7). Statistical analyses indicated that transection rats had significantly reduced BMD values when compared with the naïve and contusion groups. Correlation analyses between the BBB scores and BMD values are depicted in Figure 8B. These analyses show that the strength of association between BBB scores and BMD is strong (r = 0.774) and that the correlation coefficient is highly significantly different from zero ($p < 0.0001$). With this mineral outcome metric, we can say that 60% (0.774^2) of the variation in BMD values can be explained by mechanical unloading as represented by the decreasing locomotion function because of severity of the injury.

Table 1 shows the structural parameters of trabecular bone, including average trabecular thickness (Avg Tb.Th), average spacing (Avg Tb.Sp) between trabeculae, and trabecular number (Tb.N) per millimeter of bone length. Statistical analyses indicated that the trabecular thickness and spacing data were significantly different between the (1) naïve and contusion injury groups, and (2) contusion and transection groups. All other cross-comparisons, including the average number of trabeculae per mm of bone length, were not significant.

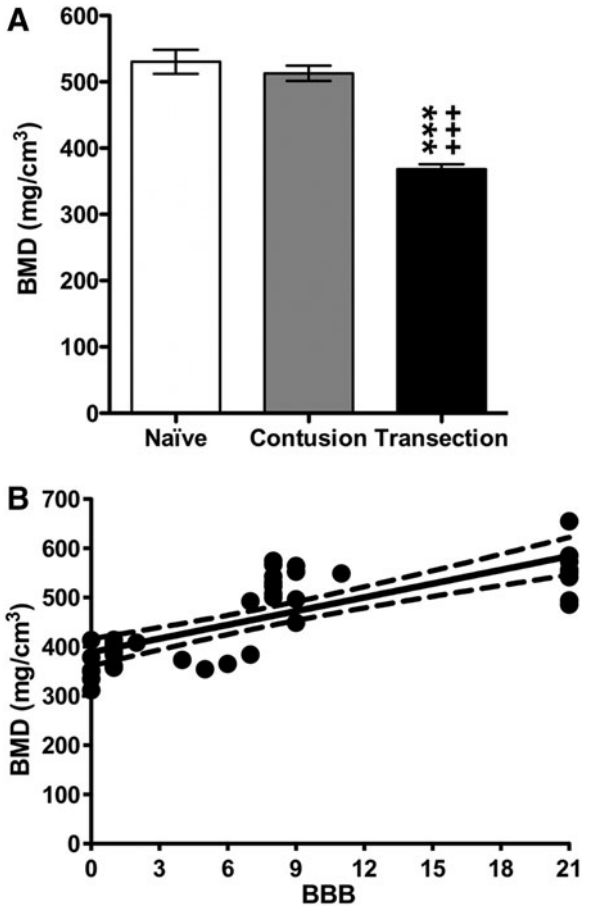

FIG. 8. (**A**) Bone mineral density (BMD, mg calcium/cm^3) determined within the trabecular bone compartment of the proximal tibia for the naïve, contusion, and transection groups (mean ± standard error of the mean). Statistical analyses (one-way analysis of variance, *post-hoc* Tukey) indicated a significant difference (*** $p < 0.005$) between the transection and naïve groups and a significant difference ($^{+++}$ $p < 0.005$) between the transection and contusion groups. (**B**) Correlation analyses between the ion groups. (**B**) Correlation analyses between the ion groups. (**B**) Correlation analyses between the Basso, Beattie, and Bresnahan (BBB) and BMD in the naïve and SCI (contusion and transection) groups. Data are presented as X-Y paired, with linear regression (solid line) and 95% confidence limits (dashed lines) of the fit.

Discussion

Little has been published regarding the loss of skeletal muscle and bone in the hindlimbs within the same rodent after SCI, and those reports have not cross-correlated sarcopenia and osteopenia

Table 1. Three-Dimensional Structural Parameters of the Trabecular Bone within the Tibial Proximal Compartment for the Naïve, Contusion, and Transection Groups*

Group	*Age (months)*	*N (animals)*	*Avg Tb.Th (μm)*	*Avg Tb.Sp (μm)*	*Tb.N (1/mm)*
Naïve	6	4	50 ± 0.5	112 ± 2	4 ± 0.1
Contusion	6	7	56 ± 2.0[a]	133 ± 8[a]	4 ± 0.2
Transection	6	11	48 ± 0.4[b]	106 ± 2[b]	5 ± 0.1

Avg Tb.Th, average trabecular thickness; Avg Tb.Sp, average spacing between trabeculae; Tb.N, trabecular number per millimeter of bone length.

*mean ± standard error of the mean.

Statistical analyses: [a]indicates $p < 0.05$ compared with naïve; [b]indicates $p < 0.05$ compared with contusion group.

with locomotor assessments. Given the increasing interest in bone-muscle interactions at both the mechanical and biochemical levels,[3] the above-mentioned issue becomes more prominent and the current study sought to thoroughly investigate it.

We have found that mechanical loading early after contusion SCI, in a state of partial paralysis (contusion SCI), can mitigate the subsequent rate of muscle and bone loss in the hindlimbs of skeletally mature rats. This is consistent with the report that incomplete SCI usually results in slower rates of bone loss than complete SCI in patients during the early or acute phase after SCI (up to four months),[8] suggesting that even partial mechanical loading of the lower extremities early after SCI can mitigate the overall rate of bone loss thereafter. In addition, it has been reported that standing or assisted walking therapy shortly after trauma may reduce the rate of bone loss in the lower extremities of patients with SCI.[20]

Our results showed that a decreased averaged myofiber CSA of both soleus and tibialis anterior muscles in the hindlimbs was correlated negatively to the level of locomotor activity. In contrast, cancellous bone loss was only significantly different in completely paralyzed rats (transection SCI). Thus, cancellous bone loss in the hindlimbs of SCI rats would appear to exhibit a threshold response, as opposed to the linear response exhibited by skeletal muscle groups in the same hindlimbs. A possible explanation for this apparent difference could be based on the mechanical and biochemical signaling between bone tissue and its surrounding skeletal muscle tissue.

We contend that partially paralyzed contusion SCI rats might have produced sufficient biochemical effectors and mechanical forces to help preserve bone tissue, while the completely paralyzed (transection SCI) rats might have been only able to produce biochemical effectors, but not sufficient mechanical forces to preserve cancellous bone tissue. We further hypothesize that these putative biochemical effectors are not sufficient to support bone mass homeostasis in the complete absence of footfall forces.

While our findings that complete paralysis leads to losses in cancellous bone BMD and BMC are generally in line with previous reports, there are some notable distinctions. Our findings cannot be directly compared with several previous studies that used young, growing rats in SCI studies.[11,12,21] The reason for this incompatibility is that studies using immature animals cannot distinguish between the negative impacts of SCI slowing or stopping bone growth from that of enhancing resorption of pre-existing bone tissue.[13] The use of skeletally mature rats to model adult human SCI effects on musculoskeletal tissues is an important factor distinguishing the current study from many in the existing literature.

The transection SCI model at the T8 level caused complete paralysis in our rats and yielded BBB scores for hindlimbs that were lower than those reported for the severe impact force group (50 g-cm, the NYU Impactor) at the T10 level in young SD rats.[12] Those authors noted that bone mass was reduced only in the 50 g-cm impact force group; all other lower impact force groups did not exhibit significant changes in bone mass (6.25, 12.5, and 25 g-cm). Thus, our findings using more skeletally mature SD rats (about six to seven months old) are consistent with those of Voor and associates,[11] who used younger, more immature rats (about six to seven weeks old). When used at 250 kDyne, the IH impactor is generating a lower impact force than what has been reported in several previous rat SCI studies (typically 25 g-cm or higher with the NYU impactor), and this low impact force may help explain why we did not observe bone loss in our contusion SCI group [12].

There was also one previous report using four-month–old female Fischer rats (nearly skeletally mature) in an SCI contusion model.[17] This study used a 10-g rod dropped from a 25-mm height applied at the T13 level to generate a near complete paralysis of the hindlimbs. Presuming that this was the case in that study, then those findings are similar to our results from the complete paralysis transection SCI model with respect to BMD and BMC evaluations. A notable exception is that the Lin and coworkers[17] study reported a large decline in cancellous bone volume fraction (BV/TV) that was not observed here. Explanations for this discrepancy between our data and this previous report regarding BV/TV might include differences in micro-CT imaging, calibration, and post-processing parameters, as well as potential differences in exact cancellous bone ROI chosen between the two studies.

Our findings are consistent with previous reports that skeletal muscle and bone mass are regulated by a variety of factors that include SCI-induced changes in mechanical loading. Future studies should examine longitudinally changes in both muscles and bone from acute through chronic SCI to more thoroughly understand adaptations in the musculoskeletal system for the purposes of developing novel and effective therapeutic strategies aimed at preventing the loss of, and/or increasing mass in, both skeletal muscles and bone after SCI.

Acknowledgments

This project was supported by National Institutes of Health (NIH) grant NS069765 and a grant from the Craig Neilsen Foundation (#297064) to Y-S. L. We would like to acknowledge Kevin Li, John Enasko and Rajaa Thalluri for their assistances in the data analyses of muscle CSA and Boris Kligman for his bone metric analyses. We would also like to acknowledge the Robotics Core at Lerner Research Institute of Cleveland Clinic for the testing of the two impact devices.

Author Disclosure Statement

No competing financial interests exist.

Reference

1. Biering-Sorensen, B., Kristensen, I.B., Kjaer, M., and Biering-Sorensen, F. (2009). Muscle after spinal cord injury. Muscle Nerve 40, 499–519.
2. Goodman, C.A., Hornberger, T.A., and Robling, A.G. (2015). Bone and skeletal muscle: key players in mechanotransduction and potential overlapping mechanisms. Bone 80, 24–36.
3. Brotto, M. and Bonewald, L. (2015). Bone and muscle: interactions beyond mechanical. Bone 80, 109–114.
4. Guo, B., Zhang, Z.K., Liang, C., Li, J., Liu, J., Lu, A., Zhang, B.T., and Zhang, G. (2017). Molecular communication from skeletal muscle to bone: a review for muscle-derived myokines regulating bone metabolism. Calcif. Tissue Int. 100, 184–192.
5. Kulshrestha, R., Chowdhury, J.R., Lalam, R.K., and Kiely, N.T. (2017). Spinal cord infarction in a sick neonate from predominant haemorrhagic aetiology: a case report. Spinal Cord Ser. Cases 3, 17038.
6. Parent, S., Mac-Thiong, J.M., Roy-Beaudry, M., Sosa, J.F., and Labelle, H. (2011). Spinal cord injury in the pediatric population: a systematic review of the literature. J. Neurotrauma 28, 1515–1524.
7. Giangregorio, L. and McCartney, N. (2006). Bone loss and muscle atrophy in spinal cord injury: epidemiology, fracture prediction, and rehabilitation strategies. J. Spinal Cord Med. 29, 489–500.
8. Garland, D.E., Adkins, R.H., and Stewart, C.A. (2008). Five-year longitudinal bone evaluations in individuals with chronic complete spinal cord injury. J. Spinal Cord Med. 31, 543–550.
9. Roberts, D., Lee, W., Cuneo, R. C., Wittmann, J., Ward, G., Flatman, R., McWhinney, B., and Hickman, P. E. (1998). Longitudinal study of

bone turnover after acute spinal cord injury. J. Clin. Endocrinol. Metab. 83, 415–422.
10. Maimoun, L., Couret, I., Mariano-Goulart, D., Dupuy, A.M., Micallef, J.P., Peruchon, E., Ohanna, F., Cristol, J.P., Rossi, M., and Leroux, J.L. (2005). Changes in osteoprotegerin/RANKL system, bone mineral density, and bone biochemicals markers in patients with recent spinal cord injury. Calcif. Tissue Int. 76, 404–411.
11. Voor, M.J., Brown, E.H., Xu, Q., Waddell, S.W., Burden, R.L., Jr., Burke, D.A., and Magnuson, D.S. (2012). Bone loss following spinal cord injury in a rat model. J. Neurotrauma 29, 1676–1682.
12. Jiang, S.D., Jiang, L.S., and Dai, L.Y. (2007). Changes in bone mass, bone structure, bone biomechanical properties, and bone metabolism after spinal cord injury: a 6-month longitudinal study in growing rats. Calcif. Tissue Int. 80, 167–175.
13. Zeng, Q.Q., Jee, W.S., Bigornia, A.E., King, J G., Jr., D'Souza, S.M., Li, X.J., Ma, Y.F., and Wechter, W.J. (1996). Time responses of cancellous and cortical bones to sciatic neurectomy in growing female rats. Bone 19, 13–21.
14. Hughes, P.C. and Tanner, J.M. (1970). The assessment of skeletal maturity in the growing rat. J. Anat. 106, 371–402.
15. Erben, R.G. (1996). Trabecular and endocortical bone surfaces in the rat: modeling or remodeling? Anat. Rec. 246, 39–46.
16. Horton, J.A., Bariteau, J.T., Loomis, R.M., Strauss, J.A., and Damron, T.A. (2008). Ontogeny of skeletal maturation in the juvenile rat. Anat. Rec. (Hoboken) 291, 283–292.
17. Lin, T., Tong, W., Chandra, A., Hsu, S.Y., Jia, H., Zhu, J., Tseng, W J., Levine, M. A., Zhang, Y., Yan, S.G., Liu, X.S., Sun, D., Young, W., and Qin, L. (2015). A comprehensive study of long-term skeletal changes after spinal cord injury in adult rats. Bone Res. 3, 15028.
18. Miller, S.C., Shupe, J.G., Redd, E.H., Miller, M.A., and Omura, T.H. (1986). Changes in bone mineral and bone formation rates during pregnancy and lactation in rats. Bone 7, 283–287.
19. Basso, D.M., Beattie, M.S., and Bresnahan, J.C. (1995). A sensitive and reliable locomotor rating scale for open field testing in rats. J. Neurotrauma 12, 1–21.
20. Dauty, M., Perrouin Verbe, B., Maugars, Y., Dubois, C., and Mathe, J.F. (2000). Supralesional and sublesional bone mineral density in spinal cord-injured patients. Bone 27, 305–309.
21. Morse, L., Teng, Y.D., Pham, L., Newton, K., Yu, D., Liao, W.L., Kohler, T., Muller, R., Graves, D., Stashenko, P., and Battaglino, R. (2008). Spinal cord injury causes rapid osteoclastic resorption and growth plate abnormalities in growing rats. Osteoporos. Int. 19, 645–652.

Address correspondence to:
Yu-Shang Lee, PhD
Department of Neurosciences
Lerner Research Institute
Cleveland Clinic
9500 Euclid Avenue
Cleveland, OH 44195

E-mail: leey2@ccf.org